On the superconductivity in hole doped cuprates

2007 J. Phys.: Condens. Matter 19 251002

(http://iopscience.iop.org/0953-8984/19/25/251002)

IOP PUBLISHING JOURNAL OF PHYSICS: CONDENSED MATTER

J. Phys.: Condens. Matter **19** (2007) 251002 (13pp) doi:10.1088/0953-8984/19/25/251002

VIEWPOINT

On the superconductivity in hole doped cuprates

K A Müller

Physik Institut, Universität Zürich, Winterthurerstrasse 190, CH-8057 Zürich, Switzerland

Received 12 February 2007
Published 30 May 2007
Online at stacks.iop.org/JPhysCM/19/251002

1. Introduction

Over two decades have passed since the discovery of superconductivity in $LaCuO_4$ [1], in which CuO_2 planes exist and for which, when it is doped with holes, the phenomenon is observed. Other cuprates have been found which contain the same CuO_2 planes and show substantially higher transition temperatures, reaching 133 K at ambient pressure [2]. Electron doping is not addressed here because of limitations on space. It is a remarkable fact that in these 20 years since the discovery of high temperature superconductivity (HTS) no other class of materials has been found which exhibits this property above the boiling point of liquid nitrogen. With a view to finding another class, it would be rewarding to understand why these exceptional properties occur, which per se are regarded as among the important unsolved problems in present day physics. It is the intention of this article to sketch experimental and theoretical results which may lead to an understanding.

2. Confirmed properties and theories

Upon doping an antiferromagnetic cuprate with holes, superconductivity sets in near 6%–7%. It increases from this critical end point in a parabolic way as a function of doping and vanishes near 20%–30%, depending on the material, with the transition temperature, T_c, or the superconducting gap, Δ_c, forming a dome; see figure 1.

The coherence lengths ξ observed in all of them are of the order of 10–20 Å, i.e. one to two orders of magnitude smaller than for a BCS material. In the latter the large ξ results from the substantial Fermi energy present in these metals, whereas in the cuprates this energy is small due to the small carrier density. The small ξ's also appear to be responsible for the very large critical magnetic fields measured [4]. These quite small ξ's remind the author of the theory of Schafroth and Blatt [5], which was competitive for BCS but was not adequate for metals; however here it comes closer to reality. Another property pertains to all of the cuprates. At optimum doping, i.e. T_c maximum, and in the normal state, the resistivity increases *linearly* with temperature [4].

According to the t–J model, carriers tunnel in a rigid AF lattice [6], and the order parameter deduced is of d-wave symmetry (see section 6), as also obtained from the RVB theory [7, 8]. This was considered to be a success. However, the T_c s deduced from these 2D models were small if they existed at all. Monte Carlo calculations did not find superconducting correlations [9]! In a more recent analytic calculation for the $d_{x^2-y^2}$ Hubbard model, no

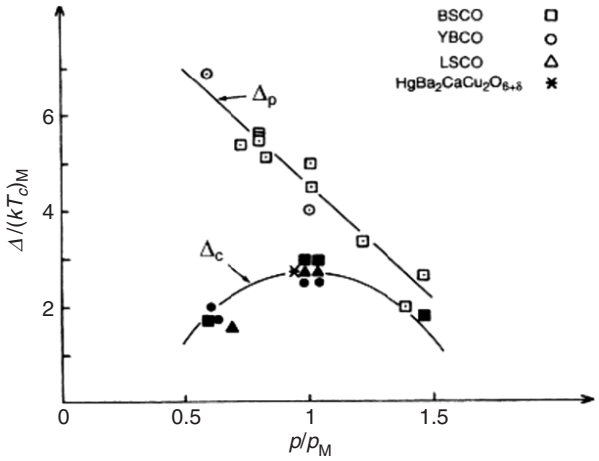

Figure 1. The superconducting gap Δ_c and pseudogap Δ_p as a function of the normalized doping density ρ/ρ_M determined from Andreev reflections [3].

long-range pairing was found at any non-zero temperature [10]. Using, instead of the single-band t–J model, a two-band model, adequate T_c's were recently obtained. In the latter a second higher band of $3r^2 - z^2$ symmetry is coupled to the lower one via *vibronic* interactions, i.e. the ions are allowed to move [11]. The latter coupling lowers the upper band to within a few meV of the lower one. This theory was initially rejected, not accepting the vibronic coupling between the two bands. This reminds the author of the famous rejection by Sir Arthur Eddington on 11 January 1935 at the Royal Astrophysical Society of the 25-year-old Chandrasekhar's calculations [12]. From them, the occurrence of 'black holes' in the cosmos was predicted. Eddington called this proposal absurd, and blocked the field for more than 35 years. In the present case the two-band model, without needing further terms or constants, also reproduces the doping dependence of the magnitude T^* of the pseudogap, which is found in all of the cuprates. Moreover, also the giant oxygen isotope effect measured for T^* and that of T_c, addressed in the next section, are obtained.

3. Isotope effects

The concept which led to the discovery of superconductivity in the cuprates was the vibronic property of the Jahn–Teller effect. Therefore looking for an isotope effect for the ligand oxygens of the Cu ions was an obvious task. The first experiment undertaken was in the group of Cardona at the MP Institute in Stuttgart. Observing vibrations perpendicular to the CuO_2 planes by means of Raman scattering, no isotope effect was found [13]. Therefore the leader of the group voiced substantial doubts at various meetings as to the vibronic character of the ground state. Subsequent systematic and site-selective studies at the University of Zürich showed to 100% the existence of isotope effects *in* the CuO_2 planes, detected by susceptibility experiments [14]; see figure 2.

These planar effects occurred from optimal doping down to the vanishing of superconductivity, pointing to polaronic character *in* the planes. The *amount* of the isotope effect increases from near zero at optimum doping down to the critical end point of superconductivity to a value *above* that of BCS theory of $\alpha = 0.5$. These data further point to an entirely different mechanism of superconductivity in the cuprates.

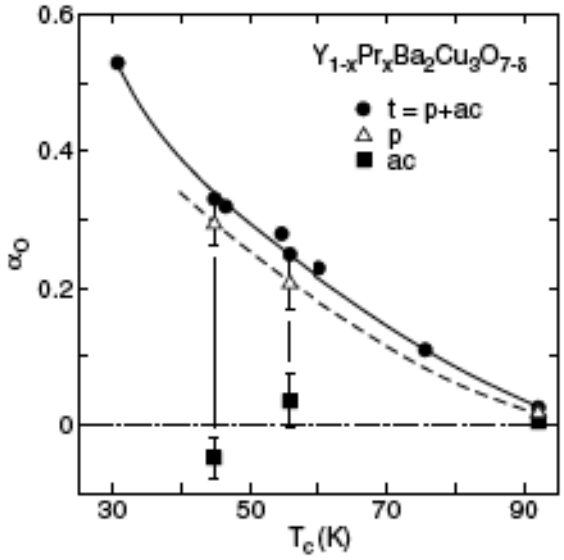

Figure 2. Total (t) and partial (p, ac) oxygen isotope exponent α_O as a function of T_c for $Y_{1-x}Pr_xBa_2Cu_3O_{7-\delta}$ (t: all oxygen sites, p: planar oxygen sites, ac: apex and chain oxygen sites). *Solid and dashed lines* are guides to the eye.

Another property of hole doped cuprates is perhaps even more astounding: the isotope effect observed for the temperature of the pseudogap T^* in the underdoped regime. It is the largest one for ^{16}O to ^{18}O substitution ever reported in any condensed matter system. It was first found using XANES (x-ray near edge absorption spectroscopy) [15], and then confirmed by means of inelastic neutron scattering [16]. In XANES the wavefunction of the x-ray-emitted electron from the Cu atom interferes with those of nearby ligands and therefore 'senses' the Cu–ligand distance. With it the Cu–O distance can be probed on a timescale of 10^{-13} s. In LSCO at T^* a change of the distance in question was detected. For a ^{16}O to ^{18}O substitution, T^* was shifted up in temperature by 110 K. Critics argued that a structural phase transition was present, which, however, is not the case.

Subsequently the enormous T^* isotope shift was confirmed using inelastic neutron scattering in YBCO [17]. In this compound Y^{3+} was replaced by Ho^{3+}, which does not alter the superconducting properties. However the Ho^{3+} ion contains 4f electrons and its 4f levels are split by the crystal field of the surrounding ions. The linewidth for the transition from the ground to the first excited state was measured. Cooling from higher temperature, a linear decrease of the width was observed, with a drop at T^* followed by a further approximately linear decrease (see figure 3) [17]. The linear decrease is attributed to a Korringa relaxation at the Ho^{3+} ion, i.e. scattering by the mobile charge carriers at the Ho^{3+} in the doped system. The drop was ascribed to the opening of the pseudogap with a reduction of carriers. Upon substituting ^{16}O by ^{18}O, the drop in relaxation, i.e. in T^*, is shifted up by 80 K.

Analogous shifts have also been found in LSCO, thus confirming these observations. It should be noted that in these linewidth experiments the timescale is of the order of 10^{-12} s, i.e., slower than for XANES. As regards the interpretation, the aforementioned vibronic band model of the previous section reproduces the isotope effect, summarized here, quite well [11]. These shifts also lead to the consequences discussed in the following paragraphs, in which the formation of bipolarons upon cooling the system through T^* is described, which does not mark a phase transition as such, but a crossover temperature.

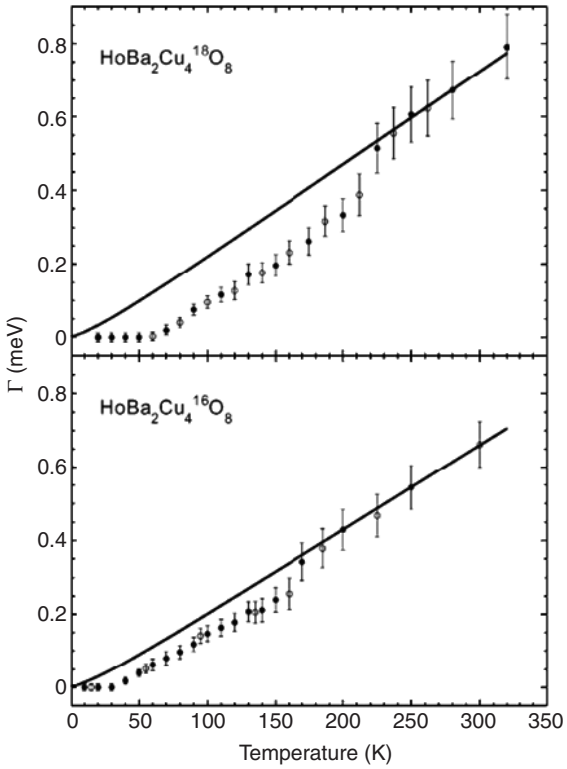

Figure 3. Temperature dependence of the intrinsic linewidth Γ (HWHM) corresponding to the Γ_3–Γ_4 ground state CF transition in $HoBa_2Cu_4\ ^{16}O_8$. The *lines* denote the linewidth in the normal state calculated from the Korringa law [17].

4. Bipolarons and fermions

The possible existence of Jahn–Teller polarons was conceived by Thomas and his group in Basilea. They used a linear molecular chain Hamiltonian to compute, using a variational method, the effective mass of the JT polaron as a function of JT coupling [18]. The outcome of the Basilean work was that the JT polaron had a very large mass. The hole doped $LaCuO_4$ and the subsequently discovered cuprate superconductors have, when undoped, all antiferromagnetic ground states of the Cu^{2+} present. A displaced JT polaron leaves behind it a string of reversed Cu spins in the relevant CuO_2 plane of the cuprates, which increases the immobility of the polaron in question. This fact added to the scepticism of the community regarding the original concept of the author. However, in 1990 in the review of Smith and Stoneham, the possible existence of bipolarons proposed by Catlow is already mentioned [19]. Thereafter, and independently, Hirsch pointed out [20] that in the case of a bipolaron, the Cu spins would remain in the AFM ground state after a bipolaron of any kind with spin zero had passed. Two years after the paper of Hirsch appeared, the important one of Alexandrov *et al* [21] was published, in which they wrote down the basic equations for the bulk properties starting from the bipolaron concept. However the temperature dependence of the susceptibility that they obtained did not fit the measured ones for certain hole dopings. It was shown by Müller *et al* [22] that the addition of a Pauli temperature independent term due to free fermions did fit the data quite well.

This meant that two types of carrier, bipolarons and fermions, were present simultaneously. A review written by Mihailovic and the author [23] on the occasion of the tenth anniversary of the discovery of the HTS emphasized the existence of two kinds of quasiparticles by demonstrating from experiments known at that time, namely magnetic susceptibility, EXAFS, pulse–probe, photoexcitation, NMR/NQR and other ones, that two components are present in cuprates. All these experimental findings have so far been ignored by the RVB and t–J community. At this point one should also emphasize that right after the HTS discovery Gorkov and Sokol [24] argued in favour of the existence of two types of particle, of fermionic and polaronic character.

More recently photoemission experiments confirmed the existence of the two quasiparticles discussed above. The dispersion of hole doped LSCO and copper whismutates showed, starting from the Fermi energy, a linear dependence as a function of the wavevector $\boldsymbol{k}$ with a knee to a further stronger linear dispersion [25]. For the former dispersion no oxygen isotope dependence was found, but for the latter it was present [26]. The occurrence of two group velocities naturally indicates the existence of two quasiparticles. The one near the Fermi energy without an isotope effect can be assigned to fermionic particles and the latter with an isotope effect to vibronic ones. It should be noted that in these experiments the wavevector direction pointed from the Γ point of the Brillouin zone to the X (π, π) point. Turning the k vector around towards the M point, the knee came closer to the Fermi energy, thus providing more spectral weight to the vibronic states.

To close this section, we should underline that the Fermi surface in the Brillouin zone as detected by means of photoemission in the whismutates [4] indicates by itself the presence of two kinds of carriers, one along the Γ–M direction, with polaronic character, and the other along the Γ–π, π direction, with fermionic character. From these findings, one is naturally interested in obtaining a more microscopic insight into the nature of the two kinds of particles present.

5. The intersite Jahn–Teller bipolaron as the generic quasiparticle

5.1. Experimental signatures for Jahn–Teller polarons

Owing to the polaronic character of the quasiparticles involved, the results from local probes are of relevance. Typical experiments sensitive to local properties are ones based on EXAFS, XANES, certain inelastic neutron scattering data, EPR, and NMR/NQR. Of importance are the time windows these techniques offer. They range from left to right for increasing windows from 10^{-13} to 10^{-6} s. The one with the shortest time window, i.e. the shortest interaction time, yields a near 'frozen' configuration of the polaron involved.

Using EXAFS the local environment around the Cu ion in the CuO_2 plane was determined by the group of Bianconi in Rome [27]: their analysis suggested two configurations. One had 'LLT' distorted octahedra and was tilted by $\sim 16°$. The latter probably arise from a sterically enlarged instantaneous Cu–O distortion. The distortions are similar to a 'Q_2' local mode, familiar from the Jahn–Teller effect. The other environment was essentially an undistorted octahedron. The distorted octahedron can be assigned to a JT polaron, whereas the undistorted one is located within a metallic cluster or stripe. This conforms with the two-particle scenario proposed above (see figure 5). The stripe formation in the CuO_2 plane shown in the upper part of the figure was deduced from x-ray experiments.

Electron paramagnetic resonance (EPR) study is another potent and relatively fast technique for probing local properties in condensed matter. An intrinsic EPR line observed for quasi-localized holes in $La_{2-x}Sr_xCuO_4$ by the group of Elschner in Darmstadt was analysed by Kochelaev *et al* [28]. The detected signal was typical for a paramagnetic centre with spin

$S = 1/2$ having axial symmetry, i.e. gyromagnetic ratios $g_\perp$ and $g_\parallel$. The parallel axis was directed perpendicular to the CuO_2 plane.

The model for the analysis of the measurements was based on the so-called three-spin polaron (3SP) proposed earlier by Emery and Reiter [29]. This polaron is created by a p hole on the oxygen atoms in the CuO_2 plane and two d holes on adjacent Cu atoms. These holes are coupled by the isotropic antiferromagnetic exchange interaction; the ground state of the 3SP has spin $S = 1/2$, in agreement with the observations. Another piece of experimental evidence for the model was the temperature dependence of the g-factors: $g_\perp$ decreases with decreasing temperature to a rather unusual value $g < 2$, and a crossover with $g_\perp$ takes place (see the inset of figure 6). Such a behaviour was consistent with dynamical Q_2 Jahn–Teller distortions of the 3SP.

5.2. The intersite Jahn–Teller bipolaron

By adding a further hole to the 3SP (figure 6), the intersite JT bipolaron is formed (figure 7).

It can be regarded as two Zhang–Rice singlets tied to each other in the lattice. One of these singlets is formed by a d hole on a Cu^{2+} ion and one p hole distributed on the oxygen ligands, of course with antiparallel p–d spins. The picture described here follows from *ab initio* calculations of Kochelaev and his group in Kazan [30]. The force which couples the two Zhang–Rice singlets is of elastic nature, and was overlooked by the t–J community. It should be noted that in contrast to the 3SP case the d spins on the two Cu^{2+} ions are *antiparallel*. Thus the Cu^{2+} spins retain the same orientation as the undoped AFM lattice. Consequently we can also regard the JT intersite bipolaron as being composed of two antiparallel p holes trapped on oxygen orbitals around two Cu^{2+} near each other.

The existence of this JT intersite bipolaron (figure 7) was first proposed by Mihailovic and Kabanov (MK) [31]. Their proposal was based on the above-described EXAFS and EPR experiments (see figures 5 and 6) and inelastic neutron scattering experiments. In the latter, Egami and collaborators measured the LO phonons in YBCO and LSCO, which exhibit a distinct feature in the dispersion at 60–80 meV that occurs in the Brillouin zone along the $\langle 100 \rangle$ wavevector [32]. The atomic displacement of this phonon was determined. On this basis, MK suggested a phenomenological interaction with a coupling constant of the form

$$g(q) = g_0[(q - q_c)^2 + \Gamma]^{-1/2} \tag{1}$$

which is resonant at the wavevector q_c. The theoretical analysis of their collaboration showed that one has couplings between $q \neq 0$ phonons and the twofold-degenerate electron states including spin, all with the resonant coupling structure of equation (1). By symmetry, there are four coupling terms. In front of each is a Pauli matrix σ_i due to the twofold degeneracy of the state. The first term results from the coupling g_0 to the breathing mode. The second and third are due to the interaction with the x^2–y^2 and xy JT modes, and the fourth, with the σ_z matrix, is due to the magnetic interaction. Measurements of the ratios of g_1 and g_2 JT coupling constants versus the magnetic coupling g_3 would settle the long-standing discussions on the importance of lattice displacements as compared to the magnetic origin of the HTS in the cuprates.

In quantum theory there are always two complementary descriptions of matter: one in terms of particles, as above, and on the other hand one in terms of waves. For the latter, the two-band model of Bussmann-Holder and Keller [11] appears a valid approach.

5.3. The phase diagram including metallic clusters or stripes, resulting from the percolation of JT bipolarons

For the intersite polaron with size l_p small but larger than the lattice scale $a, a < \xi < l_p$, superconductivity can take place through a kind of dynamic percolation. In it JT mesoscopic

pairs fluctuate and percolate coherently [33]. A quantitative development of this picture yields:

(1) an understanding of the minimum coherence length observed experimentally;
(2) the correct percentage of holes for which the onset of superconductivity is observed (6%);
(3) the correct percentage of holes (15%) for achieving the maximum value of T_c, i.e. T_c^m and T_c^m itself.

In fact, upon cooling, percolation yields extended metallic regions whose size is limited by Coulomb repulsion. The latter interaction and the JT term in the Hamiltonian have more recently been extended by adding an elastic term for the interaction of the JT bipolarons with the lattice. This term was chosen to conform with St Venat's criterion for lattice stability as first introduced by the Los Alamos group for AFMs. Depending on these interactions, clusters or stripes are formed in the CuO_2 planes. Figure 8 shows a simulation obtained *numerically*.

Depending on the elastic interaction energy chosen, in addition to clusters, stripes appear directed along $\langle 10 \rangle$ or $\langle 11 \rangle$ general directions. Earlier, the Los Alamos group had noted that $\langle 10 \rangle$ stripes exhibited metallic conduction, whereas $\langle 11 \rangle$ ones, as in doped $LaNiO_4$, are not metallic [35].

At this point it is important to be aware that the picture shown in figure 8 *is not a static one*. Pulse–probe experiments by Mihaiovic show this very clearly: in these experiments an excitation pulse is followed by a probing pulse, and the change in reflectivity R is measured as a function of time delay [36]. From the exponential decay the lifetime τ_R of a quasiparticle (QP) is obtained. Within the bipolaron pairing picture, two QPs recombine to form a bipolaron of size l_0. As a consequence, τ_R is determined by the time which acoustic phonons admit for the bipolaron volume, corresponding in a first approximation to $\tau_R = l_0 \nu_s$, where ν_s is the sound velocity. In the vicinity of T_c, l_0 is nearly the same as the coherence length ξ_0, a quite remarkable finding. Furthermore, the renormalized mean free path l_m and l_0 are also approximately the same over the entire temperature range ($T_c < T < 300$ K). The conclusion of Mihailovic [36] is: '... upon cooling, bipolarons are formed at $kT^* = 2\Delta$. They lead to a charge-inhomogeneous state. These objects form and dissociate according to thermal fluctuations, leading to a state which is *dynamically* inhomogeneous ...', in agreement with what has been outlined at the beginning of this section (figure 8). The dimensions of these objects are determined by the balance of Coulomb repulsion and lattice attraction as discussed in [36], and are of the order of $\xi_o \sim$ 1–2 nm above T_c. As the temperature is reduced, the density of pairs starts to increase and they coalesce into larger segments, which is reflected by the increasing length scales observed at low temperatures.

From the EPR data this is even true in the very underdoped regime, where superconductivity is absent. However, for doping concentrations larger than 6%, a phase percolation threshold for the metallic regions is reached, and a macroscopically phase-coherent state occurs at T_c [33].

EPR, as a local probe, has substantially underlined the existence of metallic regions in the hole doped cuprates and the essential role for the presence of bipolarons: in the low hole doping region, from 1% to 6%, Mn^{2+} was used as an EPR probe in LSCO. Two EPR lines with the same resonance frequency at $g = 2$ are detected, a narrow one and a broad one. The width of the narrow one is oxygen isotope independent, whereas the broad one is strongly isotope dependent. The narrow line was assigned to Mn^{2+} ions located in metallic regions and the broad one to those near a single polaron. Upon cooling, the narrow EPR line grows exponentially in intensity whereas the broad one nearly disappears [37]. The activation energy Δ deduced from the exponential behaviour of the narrow EPR line is 460($\pm$50) K, independent of hole doping concentration between 1% and 6%, i.e. the experimental range. The activation

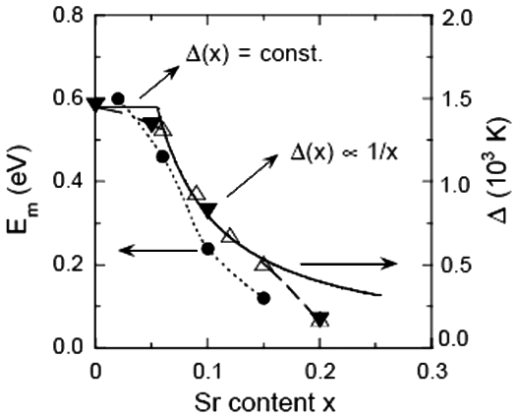

Figure 4. Composition dependence of the bipolaron binding energy Δ and $E_{\rm m} = 2g^2\hbar\omega$. The left-hand and right-hand scales are for the circle and triangle symbols, respectively. The solid triangles represent $T_{\rm max}$ values. Δ is proportional to $1/x$ for $0.06 \leqslant x \leqslant 0.15$. The results for $E_{\rm m}$ are from infrared experiments [22].

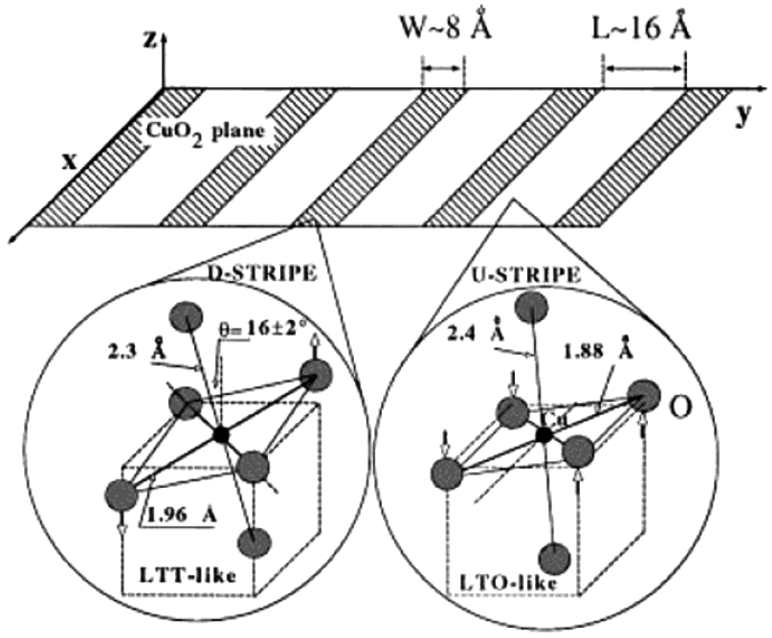

Figure 5. Stripe formation at T^* for $La_{2-x}Sr_xCuO_4$, $x = 0.15$. Pictorial views of the distorted CuO_6 octahedra (left side) of the 'LTT type' assigned to the distorted (D stripes) of width ≈8 Å and of the undistorted octahedra (U stripes) of width $L \approx 16$ Å. The superlattice of quantum stripes of wavelength $d = L + W$ is shown in the upper part [27].

energy is, within experimental error, the same as the one derived from Raman scattering (see figure 4) and inelastic neutron scattering experiments for bipolarons.

On doping LSCO above 6% holes only one Mn^{2+} EPR line is observed owing to spin diffusion effects, i.e. in the superconducting region this analysis is not applicable [37]. However, in most recent EPR experiments on Yb^{3+} substituted for Y^{3+} in YBCO an EPR line has been observed for the more highly doped material where spin diffusion is not pertinent.

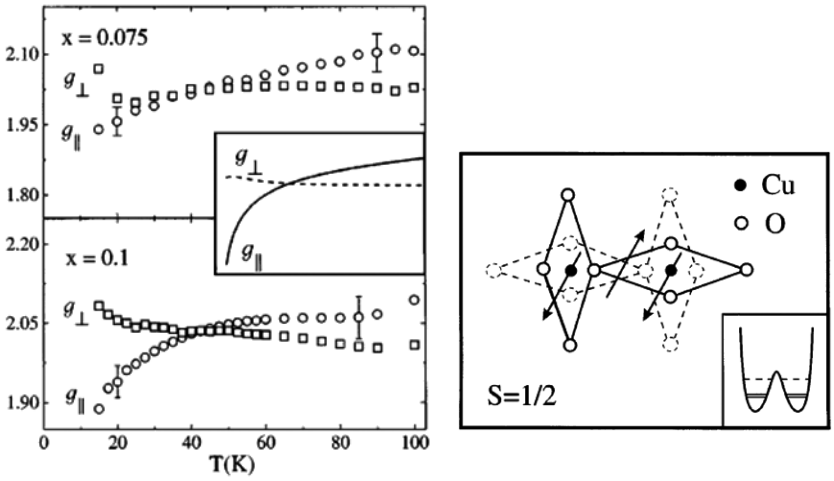

Figure 6. Right panel: the three-spin magnetic polaron which is regarded as the EPR-active centre in the CuO_2 plane. The Jahn–Teller distorted polaron has two degenerate configurations as indicated by the dashed lines. The inset shows the corresponding double-well potential with the excited vibronic states (dashed lines) and the ground state split by tunnelling (solid lines) [28]. Left panel: temperature dependence of the g-factors for two different doping concentrations. The inset shows the results obtained from model calculations based on the 3SP of the right panel.

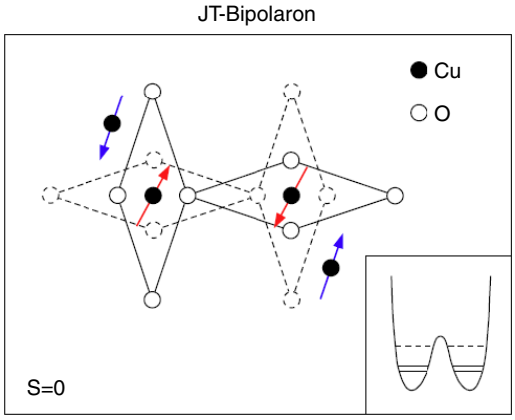

Figure 7. Schematic representation of the intersite Jahn–Teller bipolaron.
(This figure is in colour only in the electronic version)

The above finding has a macroscopic consequence as well, because the EPR intensity follows the same temperature dependence as the in-plane resistivity anisotropy in LSCO for the same doping range (figure 8) [38]. This same temperature behaviour of the microscopic EPR and the macroscopic resistivity anisotropy as shown in figure 9 is astounding. *This result suggests that bipolarons are the microscopic entities responsible for the formation of metallic clusters or stripes to which the observed resistivity anisotropy has been attributed* [38]. The bipolaron formation can then be the origin of the formation of hole-rich regions, by attracting additional holes via elastic coupling forces, as outlined in relation to the simulations shown in figure 8. Because of the high anisotropy of the elastic forces, these regions self-organize into

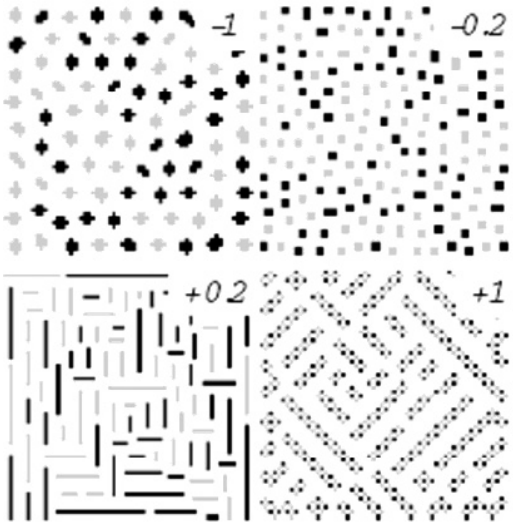

Figure 8. Snapshots of the simulations for $t = 0.2$ and $v_l(1,0)$ as a function of $v_l(1,1)$, where t is the reduced temperature, n is the density and $v_l(1,0)$, $v_l(1,1)$ stand for the short-range nearest and next nearest neighbour interactions [34].

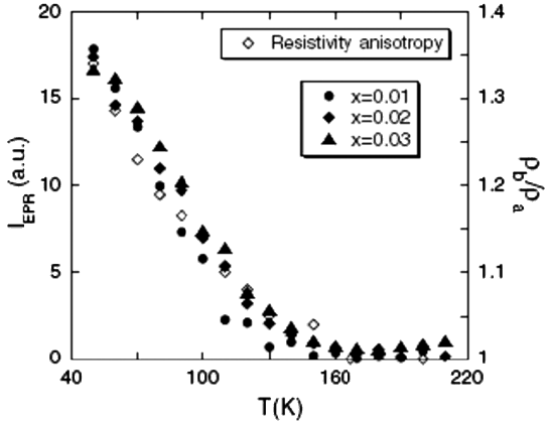

Figure 9. Temperature dependence of the narrow EPR line intensities for $La_{2-x}Sr_xCu_{0.98}Mn_{0.02}O_4$ and the resistivity anisotropic ratio of $La_{1.97}Sr_{0.03}CuO_4$ [37].

dynamical stripe patterns. Therefore, the bipolaron formation energy Δ can also be regarded as an energy scale for the onset of stripe formation associated with the pseudogap temperature T^*. Following the theory of Alexandrov, Kabanov and Mott and the experimental findings as reproduced in figure 4, the bipolaronic formation energy Δ is substantially reduced with doping x towards maximum T_c. The bipolarons overlap considerably, and the scenario for bipolarons described ceases to be valid near optimum doping. The aforementioned mean field two-band theory [11] describes the behaviour of the doped cuprates better.

6. The symmetry of the superconducting wavefunction

The classical superconductors of metallic or intermetallic kind all show so-called s-type symmetry of their superconducting macroscopic wavefunction, i.e. the gap opens symmetrically in all directions in wavevector space. This gap may show some anisotropy if the superconductor's lattice deviates substantially from cubic symmetry. The case of the HTS is quite different. Because of the layered structure, interest has mainly been focused on the behaviour of the gap observed parallel to the CuO_2 planes. Here the 2D, RVB and t–J models

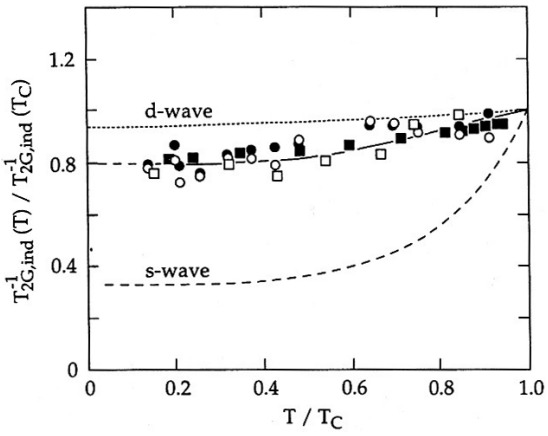

Figure 10. Temperature dependence of $T_{2G,\mathrm{ind}}^{-1}$ at copper sites in the superconducting state. The dashed and dotted lines are theoretical curves from Bulut and Scalapino. The various symbols are from data obtained at the University of Zürich NMR group [41].

predicted a d-wave symmetry gap quite early on, in which the full gap occurs along the ⟨10⟩ and ⟨01⟩ general directions, whereas it vanishes along the ⟨11⟩ ones [6, 7].

The efforts to determine the symmetry of the wavefunction in HTS have been very intensive. In the course of time the outcome, led after tunnelling experiments to the famous tri-crystal experiments at IBM, and was in favour of d-wave symmetry [38]. However, there were still experiments which indicated the presence of a non-vanishing s-wave percentage, i.e. a gap in the ⟨11⟩ directions at low temperatures. The present author then recognized that all experiments indicating pure, i.e. up to 100%, d-wave symmetry resulted from experiments in which the surface was involved, such as tunnelling, photoemission ones etc, whereas bulk sensitive experiments showed a non-vanishing s-wave contribution [40].

To reveal the above in the results acquired, we refer to $1/T_2$ NMR in YBCO data obtained at the University of Zürich. In a review on the occasion of the 10th anniversary of the discovery of HTS, it was shown that the $1/T_2$ data lay *in between* the ones computed for pure d-wave and pure s-wave symmetry [41].

Interpolating linearly between the theoretical curves in figure 10, a 20%–25% s character was obtained. Most remarkably, in very muon spin rotation experiments on LSCO, in which the London penetration lengths λ_{ab} were measured as a function of temperature, two gaps were found, one having s-wave character and the other d-wave character. The amount of s is again 20%–25% in low magnetic field [42]! Furthermore the linewidth of the transition from the ground to first excited level of the probing Ho^{3+} in YBCO (see figure 3) has a turning tangent in the range $T_c < T < T^*$. The latter behaviour has been modelled with the temperature dependence of the Fermi arc detected by means of photoemission, and a 25% s-wave plus a 75% d-wave contribution was observed [43]. In this experiment the symmetry is deduced from the range above T_c. This means that one experiment on YBCO above T_c and two on the superconducting phase in LSCO and YBCO yield the same proportion of s-wave and d-wave contents *for the bulk.* On the other hand, *surface sensitive* experiments yield near 100% d-wave symmetry [39].

This important difference is a consequence of the symmetry breaking present at the superconducting/vacuum interface. It was emphasized by the group of de Gennes over three decades ago for the quantum liquid ^{4}He [44], and pointed out to be present for superconductors

by Iachello [43]. So why is it not observed in the classical superconductors? In the latter the coherence length ξ is substantial, of the order of 100 to 1000 Å, and the thin surface layer of different symmetry appears not weighted sufficiently in the experiments. In contrast, for the HTS materials with their small ξ, of the order of 10 Å, the different symmetry near the surface is sensed. In another respect, the small ξ makes it possible to observe critical phenomena, say at the critical end point occurring at the onset of superconductivity with doping, or in specific heat data near T_c, whereas in classical superconductors mean field behaviour is observed, in all of them [46].

7. The role of antiferromagnetism

The undoped cuprates are—without exception—insulating antiferromagnets. The AFM interaction forms the basis of the RVB and t–J models. Thus, why has this interaction not been addressed in more detail in this Viewpoint, and why did AFM not appear relevant in most of the experiments discussed? First, it is important to realize that superconductivity occurs for a small doping range. Therefore probing the AFM, say using neutron scattering, the *heterogeneous* regions in the lattice where the charges are located remain undetected. Of importance also is an overlooked theoretical finding of the group of Bishop of over a dozen years ago [35]: if metallic stripes are present in a cuprate plane, the AFM interaction is reduced to a substantial degree, and it nearly vanishes, upon approaching a conducting metallic stripe. This is very likely also the case for the single bipolarons, which agglomerate to form clusters. The latter are of course separated by AFM near insulating material through which the carriers in the metallic stripes or clusters can tunnel. But one may then ask whether the insulating property is more relevant than the AFM one. If the former is the case then the search for a new HTS class can be extended to inert oxides, where the polarizability of the oxygen ions is relevant. In this context the recent theoretical paper by Kresin and Ovchinnikov is of interest [47]. These authors find considerably enhanced T_c's for mesoscopic clusters, i.e. zero-dimensional superconductivity. Tunnelling between these clusters then induces bulk, 3D, enhanced superconductivity by establishing phase coherence, as was discovered almost three decades ago in granular aluminium [48].

Acknowledgment

The author thanks Marshall Stoneham for inviting him to write his Viewpoint.

References

[1] Bednorz J G and Müller K A 1986 *Z. Phys.* B **64** 189
Bednorz J G and Müller K A 1988 *Adv. Chem.* **100** 757 (Nobel Lecture)
[2] Schilling A, Cantoni M, Goa J D and Ott H R 1993 *Nature* **337** 56
[3] Deutscher G 1999 *Nature* **397** 410
[4] See Kuzmany H, Mehring M and Fink J (ed) 1992 *Electronic Properties of High-T_c Superconductors* (*Springer Series in Solid-State Sciences* vol 113) (Berlin: Springer)
[5] Schafroth M R and Blatt J M 1955 *Phys. Rev.* **100** 1921
[6] Zhang F C and Rice T M 1988 *Phys. Rev.* B **37** 3758
[7] Zhang F C, Gross C, Rice T M and Shiba H 1988 *Supercond. Sci. Technol.* **1** 36
[8] Gross C 1988 *Phys. Rev.* B **39** 931
[9] Morgenstern I 1988 *Z. Phys.* B **70** 291
[10] Su G and Suzuki M 1998 *Phys. Rev.* B **58** 117
[11] Bussmann-Holder A and Keller H 2005 *Eur. Phys. J.* B **44** 487
Bussmann-Holder A and Keller H 2007 *Polarons in Advanced Matter* ed A S Alexandrov (Berlin: Springer) at press

[12] Miller A I 2006 *Empire of the Stars* Abacus p 7
[13] Cardona M, Liu R, Thomsen C, Kress W, Schönherr E, Bauer M, Genzel L and König W 1988 *Solid State Commun.* **67** 789
Thomsen C, Mattausch Hj, Bauer M, Liu R, Genzel L and Gardona M 1988 *Solid State Commun.* **67** 1069
[14] Zech D, Keller H, Conder K, Kaldis E, Liarokapis E, Poulakis N and Müller K A 1994 *Nature* **371** 681
[15] Keller H 2005 *Structure and Bonding* vol 114, ed K A Müller and A Bussmann-Holder (Berlin: Springer) p 143
[16] Lanzara A, Zhao G M, Saini N L, Bianconi A, Conder K, Keller H and Müller K A 1999 *J. Phys.: Condens. Matter* **11** L541
[17] Furrer A 2005 *Structure and Bonding* vol 114, ed K A Müller and A Bussmann-Holder (Berlin: Springer) p 171
[18] Höck K H, Nickisch H and Thomas H 1983 *Helv. Phys. Acta* **56** 237
[19] Stoneham A M and Smith L W 1990 *J. Phys.: Condens. Matter* **3** 225
[20] Hirsch J E 1993 *Phys. Rev.* B **47** 5351
[21] Alexandrov A S, Kabanov V V and Mott N F 1996 *Phys. Rev. Lett.* **77** 4796
[22] Müller K A, Zhao G M, Conder K and Keller H 1998 *J. Phys.: Condens. Matter* **10** L291
[23] Mihailovic D and Müller K A *High-T_c Superconductivity 1996: Ten Years after the Discovery* (*NATO ASI Ser.* vol 343) (Dordrecht: Kluwer)
[24] Gor'kov L P and Sokol A V 1987 *JETP Lett.* **46** 420
[25] Lanzara A, Bogdanov P V, Zhou X, Kellar S A, Feng D I, Liu E D, Yoshida T, Eisaki H, Fujimori A, Kishio K, Shimoyama J L, Noda T, Uchida S, Hussain Z and Shen Z X 2001 *Nature* **412** 510
[26] Gweon G H, Sasagawa T, Zhou S Y, Graf J, Tagaki H, Lee D H and Lanzara A 2004 *Nature* **430** 187
[27] Bianconi A, Saini N L, Lanzara A, Missori M, Rosetti T, Oyanagi H, Yamaguchi H, Oka K and Itoh T 1996 *Phys. Rev. Lett.* **76** 3412
[28] Kochelaev B J, Sichelschmidt J, Elschner B, Lemor W and Loidl A 1997 *Phys. Rev. Lett.* **79** 4274
[29] Emery V J and Reiter G 1988 *Phys. Rev.* B **38** 4547
[30] Kochelaev B, Safina A M, Shengelaya A S, Müller K A and Conder K 2003 *Mod. Phys. Lett.* B **17** 415
[31] Kabanov V V and Mihailovic D 2000 *J. Supercond.* **13** 959
Mihailovic D and Kabanov V V 2001 *Phys. Rev.* B **63** 054505
[32] McQueeny R J, Petrov Y, Egami T, Yethiraj M, Shirane M and Endoh Y 1999 *Phys. Rev. Lett.* **82** 628
Petrov Y, Egami T, McQueeny R J, Yethiraj M, Mook H A and Dogan F 2000 *Preprint* cond-mat/400034
[33] Mihailivic D, Kabanov V V and Müller K A 2002 *Europhys. Lett.* **57** 254
[34] Mertelj T, Kabanov V V and Mihailivic D 2005 *Phys. Rev. Lett.* **94** 147003
[35] Yu Z G, Zang J, Gammel J T and Bishop A R 1998 *Phys. Rev.* B **57** R3241
[36] Mihailovic D 2005 *Phys. Rev. Lett.* **94** 207001
[37] Shengelaya A, Brun M, Kochelaev B J, Safina A, Conder K and Müller K A 2004 *Phys. Rev. Lett.* **93** 017001
[38] Ando Y, Segawa K, Komiya S and Lavrov A N 2002 *Phys. Rev. Lett.* **88** 137005
[39] Tsuei C C and Kirtely J R 2002 *Rev. Mod. Phys.* **72** 289
[40] Müller K A 2002 *Phil. Mag. Lett.* **82** 270
Applied Superconductivity 2003 (*Inst. Phys Conf. Series* vol 181) p 3
[41] Müller K A and Keller H 1996 *High-T_c Superconductivity 1996: Ten Years After the Discovery* (*NATO ASI Ser. E* vol 343) (Dordrecht: Kluwer)
[42] Kasanov R, Shengelaya A, Maisuradze A, La Mattina F, Bussmann-Holder A, Keller H and Müller K A 2007 *Phys. Rev. Lett.* at press
[43] Furrer A 2007 at press
[44] Ambegokar V, deGennes P G and Rainer D 1974 *Phys. Rev.* A **9** 2676
[45] Iachello F 2006 *Symmetry and Heterogeneity of High-T_c Superconductors* (*NATO Sciences Series II* vol 214) (Berlin: Springer) pp 165–80
[46] Schneider T and Singer J M 2000 *Phase Transition Approach to High Temperature Superconductivity* (London: Imperial College Press)
[47] Kresin V Z and Ovchinnikov Y N 2006 *Phys. Rev.* B **74** 02514
[48] Deutscher and Dodds S A 1977 *Phys. Rev.* B **16** 3936